# A Waveguide Polarisation Toolset Design based on Mode-Beating

**David C. Hutchings,** ***Senior Member, IEEE*****, Barry M. Holmes,** ***Member, IEEE***

*School of Engineering, University of Glasgow, Glasgow G12 8QQ, Scotland, U.K.*

*DOI: 10.1109/JPHOT.2011.XXXXXXX*


Manuscript received XXX, 2011; revised XXX, 2011. First published XXX, 2011. Current version published XXX, 2011.

**Abstract:** A toolset of waveguide elements is examined which can be combined to produce polarisation functional devices in a single contiguous waveguide. In particular waveguide implementations of an optical isolator and a polarisation modulator are discussed. The waveguide elements: quasi-phase-matched nonreciprocal polarisation mode converter, reciprocal polarisation mode converter and a differential phase shifter, are all based on mode-beating. A universal 3 dB reciprocal polarisation mode converter specification is identified which suffices for all the polarisation functional devices considered here. A full-vectorial modesolver is used to determine the modes in a number of example III-V waveguide structures and the polarisation state evolution is considered by using an averaged Stokes vector illustrated on the Poincaré sphere construct.

**Index Terms:** Integrated Photonic Systems, Waveguide devices, Polarisation, Magnetophotonics, Electro-optic modulation.

## 1. Introduction

The optical polarisation state and its control is becoming of increasing concern in the telecommunications field. First, the polarisation state is normally employed in non-reciprocal elements, for example optical isolators to suppress back-reflections to protect optical sources and other devices from injection noise, or optical circulators to route counter-propagating signals in a single physical channel to different ports. Second, the polarisation state provides an additional degree of freedom and with a suitable multiplexer/demultiplexer technology the capacity of a link can be increased. Third, with an increasing polarisation sensitivity to a network with increasing data rates and polarisation dependent components, such as semiconductor optical amplifiers and photonic integrated circuits, it is becoming essential that the polarisation state can be detected and modified.

Manipulating the polarisation state is also a route to amplitude modulation of light by using an analyser, or other polarisation selective element, in the system. By integrating the modulator with the laser source the alignment of components is ensured, yet it avoids the disadvantages of direct modulation of diode lasers.

Current solutions to polarisation-based applications generally make use of bulk components. These are waveplates or retarders (usually as quarter- or half-waveplates), polarisers or polarising beam splitters, and bulk magneto-optic crystals (usually from the yttrium iron garnet family). In many applications the polarisation state is adjusted by mechanically rotating the wave plate or by employing a Pockel's electro-optic cell. The consequence of using bulk components to build optical systems is that the assembly and alignment of the components limits production volumes,

affects reproducability and yield, and becomes a major part of the overall manufacturing cost. On the other hand, photonic integration has proved technically successful in developing techniques for combining multiple optical devices onto a single chip with the benefits of added functionality, and reduction in costs, arising from the replacement of manual assembly and alignment of individual components with lithographic techniques. There are added advantages arising from the miniaturisation, such as the use of *p-i-n* junctions to concentrate the application of an electric field to the depletion layer and greatly reduce the drive voltage required for electro-optic modulation, for example, using the quantum confined Stark effect (QCSE). The area of polarisation agility, control and functionality is, however, relatively undeveloped within photonic integration platforms. The object of this paper is to discuss and analyse a toolkit of component elements to provide additional functionality through the manipulation of the polarisation state of light.

## 2. Guided Mode Analysis

In this paper we will restrict consideration to waveguides that are conventionally termed *single-moded*, normally used to denote waveguides which support just two mutually orthogonally polarised, single-lobed guided modes $\Psi_{n1}(x,y)$ and $\Psi_{n2}(x,y)$ [1]. We will consider an optical system or a integrated waveguide device to consist of a sequence of optical waveguide elements where the optical loss to radiation modes and reflections at each transition can be neglected or treated as an averaged global loss. This is appropriate where there has been a designed mode-matching between consecutive elements, or where there is a graded transition region, for example by incorporating a tapered section [2], [3]. This allows the light propagating in each element to be expressed as a linear combination of the guided modes $a_n\Psi_{n1}(x,y)+b_n\Psi_{n2}(x,y)$. The coefficients $a_n$ and $b_n$ are, in general, complex and can be related to those in an adjacent waveguide element through a unimodular transfer matrix. Now, as these modes will be associated with propagation constants $\beta_{n1}$ and $\beta_{n2}$ respectively, due to mode beating the propagation evolution of the guided wave within an element will be oscillatory with a periodic length $2L_{1/2}$, where,

$$L_{1/2} = \frac{\pi}{|\beta_{n1} - \beta_{n2}|} \tag{1}$$

This paper uses the axes definition that the $z$-direction is parallel to the waveguides, and takes the $x$- and $y$-axes to be in the plane and perpendicular to the plane of the wafer respectively. The guided wave at a point $(x,y,z)$ can be represented in terms of the Stokes parameters calculated using the transverse field components:

$$\begin{aligned} S_0(x,y) &= |H_y|^2 + |H_x|^2 \\ S_1(x,y) &= |H_y|^2 - |H_x|^2 \\ S_2(x,y) &= 2\mathrm{Re}(H_y H_x^*) \\ S_3(x,y) &= 2\mathrm{Im}(H_y H_x^*) \end{aligned} \tag{2}$$

Here we express the Stokes parameters in terms of the transverse magnetic field components $H_x(x,y)$ and $H_y(x,y)$. These are normally the direct output of full-vectorial modesolvers, and can be used to compute all other field components ($H_z$, $E_x$, $E_y$ and $E_z$). At each point the relation $S_1^2 + S_2^2 + S_3^2 = S_0^2$ is satisfied and consequently the Poincaré sphere (Fig.1) provides a useful graphical representation of the polarisation state.

Now for the guided modes in single-moded rib and strip-loaded waveguides, the polarisation state, which can be represented by the normalised Stokes vector $(S_1,S_2,S_3)/S_0$, typically remains close to uniform over the transverse area of the mode that carries nearly all the power of the mode. This can be seen in the rib waveguide example shown in Fig.2 calculated using the full-vectorial finite-difference modesolver of Fallahkhair et al [4] The contour lines are at 5 dB intervals ranging from 0 (the peak value for the mode) to -35 dB. $S_3$ is zero over these transverse mode profiles, and the peak value of $S_2$ is at least 15 dB below the peak value for $S_1$. Although these modes

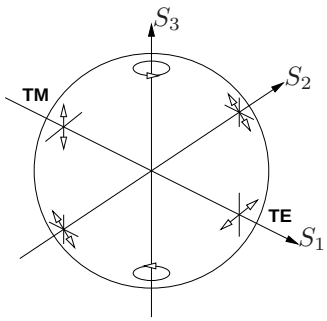


Fig. 1. The Poincaré sphere can be used to represent the polarisation state on the surface of a sphere in the Stokes vector space. Linear polarisation states lie on the equator and circular polarisation states at the poles.

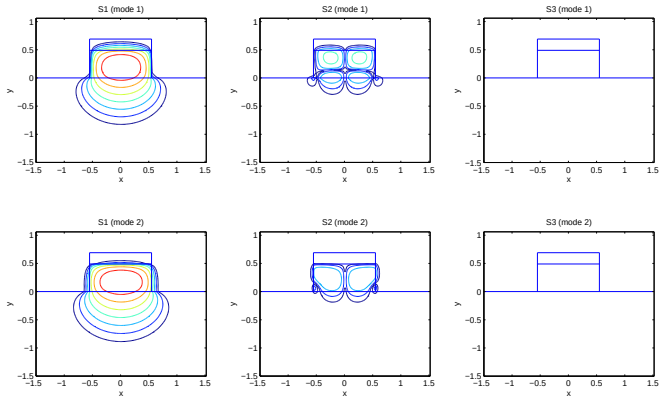


Fig. 2. The modulus of the Stokes parameters for the two guided modes at a wavelength of $\lambda$ =1.064 $\mu$m calculated using a full-vectorial modesolver. The 1.1 $\mu$m wide rib is composed of 0.49 $\mu$m thick GaAs on a $Al_{0.27}Ga_{0.73}As$ lower cladding with a 200 nm $SiO_2$ cap.

are technically hybrid, they are routinely referred to as “TE” ($S_1 > 0$, effective index $n_{\text{eff}}$ =3.3670) and “TM” ($S_1 < 0$, effective index $n_{\text{eff}}$ =3.3592) modes respectively. The corresponding half-beat-length is therefore 68.29 $\mu$m.

If we are able to neglect the transverse variation in polarisation state for each mode, then it suffices to condense the Stokes vectors to normalised, averaged values,

$$\overline{S}_j = \frac{\iint S_j(x,y)\,\mathrm{d}x\,\mathrm{d}y}{\iint S_0(x,y)\,\mathrm{d}x\,\mathrm{d}y} \qquad j = 1,2,3 \tag{3}$$

For the example rib waveguide this provides values $\overline{\mathbf{S}}$ =(0.9994,0,0) and (-0.9997,0,0) for the two modes respectively. The applicability of this approximation can be gauged by the deviation of the modulus of the normalised, averaged Stokes vector from unity.

By condensing the polarisation state of a guided wave to a single Stokes vector, it allows plane-wave constructs to be employed. In particular the Poincaré sphere allows the polarisation state to be represented as a single point on a sphere of unit radius. Two modes will be represented by two diametrically opposite points on the Poincaré sphere and the axis through them corresponds to the optic axis. The evolution of the polarisation state can be expressed as

$$\frac{\mathrm{d}S_j}{\mathrm{d}z} = -\mathrm{i}\,\{S_j, H\} \tag{4}$$

where $\{,\}$ denotes the Poisson bracket. The cyclical relation between the Stokes parameters can be expressed as

$$\{S_j, S_k\} = 2\mathrm{i}\epsilon_{jkl}S_l \tag{5}$$

where the alternator $\epsilon_{jkl}$ is equal to $+1$ for a cyclic permutation, $-1$ for anticyclic and zero otherwise. The polarisation Hamiltonian depends on the contributions to the birefringence and the orientation of the modal axis. In the symmetric waveguide example in Fig.2 the modal axis is the $S_1$ axis and the polarisation Hamiltonian is given by

$$H = \frac{1}{2}\Delta k_{\mathrm{brf}} S_1 \tag{6}$$

where $\Delta k_{\mathrm{brf}} = 2\pi\Delta n_{\mathrm{eff}}/\lambda$. The evolution of a guided wave due to mode-beating transcribes a path of constant Hamiltonian, which corresponds to a simple rotation around the modal axis of the Poincaré sphere.

## 3. Polarisation Elements for a Planar Waveguide Platform

### 3.1. Nonreciprocal Polarisation Mode Convertor

YIG and related garnets are overwhelmingly suited to magneto-optic effects in propagation with a large Verdet constant and low optical loss in the near-IR, but have refractive indices substantially lower than the III-V semiconductor materials used in laser diodes. In order to effectively guide light, the refractive index of the core layer must normally be greater than that of the cladding layers. This, therefore, normally precludes the incorporation of conventional MO materials as waveguide core layers in III-V structures. However, this dichotomy may be circumvented through the integration of the MO media as an upper cladding layer [5], [6].

Fig.3 shows the modulus of the Stokes parameters for the guided modes of the GaAs/AlGaAs waveguide example shown in Fig.2, but with the substitution of the silica cap layer with a transparent magneto-optic film. The full-vectorial finite-difference modesolver [4] is formulated for anisotropic dielectric tensors that enable the incorporation of complex off-diagonal elements appropriate to magneto-optics. The 200 nm thick magneto-optic upper cladding is taken to have $n$ =2.19 (garnet) and $\varepsilon_{xy}$ =0.10i corresponding to a longitudinal magnetic field (parallel to the propagation direction). The consequence of the Faraday rotation in the magneto-optic cladding is to modify the guided modes such that they now have a significant $S_3$ component. Upon reversing the direction of the applied magnetic field, the sign of the $S_3$ component changes. The averaged Stokes parameter vector for each of the two guided modes is rotated from the $S_1$ axis towards the $S_3$ axis: $\overline{\mathbf{S}}$ =(0.9990,0,-0.0316) and (-0.9981,0,0.0566) with effective indices $n_{\mathrm{eff}}$ =3.3689 and 3.3630 respectively, giving a half-beat length of 90.36 $\mu$m.

Note that in this example the averaged Stokes parameter vector for the two guided modes are not quite diametrically opposite on the Poincaré sphere representation. This is because the TM-like mode has a somewhat larger component within the magneto-optic cladding than the TE-like mode due to the substantive index difference between the semiconductor and the garnet layers and the boundary conditions for the tangential field, $E_x$, and normal flux density, $D_y$, at the interface. Consequently, while the evolution of the averaged Stokes parameter vector will transcribe an orbit centred around a mode in the vicinity of that mode, the evolution orbits will deviate slightly from concentricity across extent of the Poincaré sphere.

The injection of a TE-polarised guided wave $\overline{\mathbf{S}}$ =(1,0,0) into such a section will give rise to mode-beating. However, as the evolution of the averaged Stokes parameter vector is an orbit around the modal point, there is only limited conversion in the development of a TM-polarised component after a half-beat-length. This is a consequence of the inherent structural birefringence usually associated with planar waveguide format and has long been recognised as a fundamental limitation of waveguide isolators based on Faraday rotation.

Such a limitation is a general issue for coherent mode conversion processes (which also include nonlinear frequency generation) where substantive conversion requires matching the phase

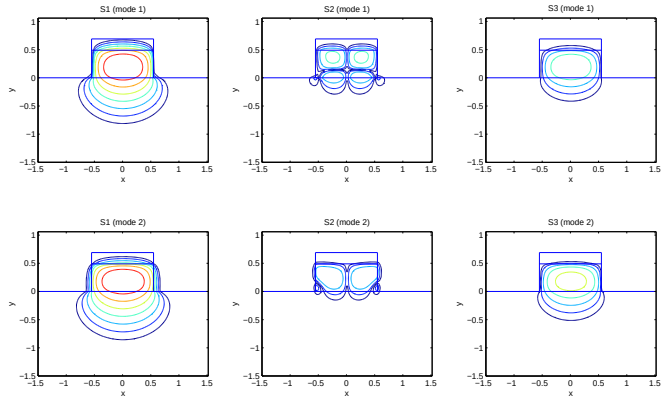


Fig. 3. The modulus of the Stokes parameters for the two guided modes at a wavelength of $\lambda$ =1.064 $\mu$m calculated using a full-vectorial modesolver. The rib waveguide structure is identical to Fig.2 except with the replacement of the silica cap with a 200 nm thick magneto-optic upper cladding.

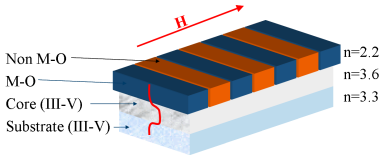


Fig. 4. Schematic of quasi-phase-matched Faraday rotation waveguiding structure with an alternating upper cladding of magneto-optic (blue) and dielectric (orange).

velocities of the modes concerned. An alternate strategy to achieving perfect phase-matching is quasi-phase-matching [7] (QPM) where the structure is periodically modified to maintain a monotonic conversion process. In the case of nonreciprocal polarisation conversion by Faraday rotation the equivalent of domain reversal over a limited number of periods has been demonstrated by using a serpentine current [8] and by using a garnet structural modification with laser annealing [9]. The evolution of the averaged Stokes parameters would approximately follow a sequence of half-orbits alternating between rotation axes along the directions $(\Delta k_{\mathrm{brf}}, 0, \pm\Delta k_{\mathrm{MO}})$ [5], [9].

It would be challenging to extend these domain reversal techniques to short coherence lengths with a large number of periods due to issues with demagnetisation and edge effects between the oppositely magnetised sections. Another strategy is to use an alternating sequence of magneto-optic and non-magneto-optic materials [10]. This could be accomplished by patterning of a garnet upper cladding, and deposition of a dielectric film of similar refractive index (or vice versa), as shown in Fig.4. Here the evolution of the averaged Stokes parameters would approximately follow a sequence of half-orbits alternating between rotation axes along the directions $(\Delta k_{\mathrm{brf}}, 0, \Delta k_{\mathrm{MO}})$ and $(\Delta k_{\mathrm{brf}}, 0, 0)$. Although the example waveguide profiles shown in Fig.2 and 3 have a significant refractive index difference between the upper cladding media (silica versus garnet), the difference in the calculated effective indices for the modes is only 0.002–0.004 which indicates that scattering at the section interfaces should not be a concern, especially as the conditions for Bragg scattering are highly unlikely to be satisfied. Therefore the use of an alternating upper cladding is somewhat tolerant of the refractive index differences of the upper claddings.

### *3.2. Reciprocal Polarisation Mode Convertor*

For an integrated waveguide isolator based on Faraday rotation, while it is possible to devise polarisation selectivity for TE- or TM-polarised modes, it is not straightforward to replicate this

selectivity for a specifically orientated polariser, including the desired 45° orientation. One solution is to additionally incorporate a reciprocal polarisation mode converter (R-PMC) section, which provides the functionality of an appropriately orientated waveplate [5]. Such R-PMCs can also be exploited in a range of other applications from mode-conversion (e.g. for polarisation diversity formats and polarisation independent functionality), to splitters and combiners (e.g. in modulators). The mode-beating approach to R-PMC uses a waveguide with an asymmetric cross-section [11] where the modes contain both significant TE- and TM-components.

A common approach to the fabrication of a semiconductor rib waveguide with an asymmetric cross-section is to use a combination of dry-etch and an anisotropic wet-etch for the two waveguide walls [12], [13]. Asymmetric profiled waveguides fabricated with a single-step dry-etching have been demonstrated using a spatially anisotropic etch [14], using an angled substrate holder [3], or using reactive ion etch (RIE) lag phenomena with offset trenches [2] or a single trench [15]. The RIE lag approach is particularly attractive as the sub-wavelength features can be tapered to provide smooth transitions between waveguide elements.

The majority of interest in mode-beating R-PMCs has focussed on waveguide profiles that can provide 100% TE- to TM-polarisation conversion in a half-beat-length, i.e. the equivalent of a bulk birefringent element with an optic axis orientated at 45° to the wafer normal. Such a waveguide solution can only be approached asymptotically with increasing stringent tolerance requirements on the cross-sectional profile [15]. The same stringent profile requirements also apply for the implementation of a 50% mode conversion with exactly a quarter-beat-length element.

We have identified that most polarisation functionality can be implemented with a waveguide element providing 50% TE- to TM-polarisation conversion in a half-beat-length, although consequently multi-element devices may be necessary. This waveguide element is the equivalent of a bulk birefringent half-waveplate with an optic axis orientated at 22.5° or 67.5° to the wafer normal. The Stokes vectors corresponding to these optic axis orientations are $\mathbf{S} = (1/\sqrt{2}, \pm 1/\sqrt{2}, 0)$ and $(-1/\sqrt{2}, \pm 1/\sqrt{2}, 0)$ respectively. This element is a modal 3 dB splitter where a singly polarised guided wave input produces equally split power output into the two output polarisation modes with a relative phase of 0 or 180°. Unlike the 100% conversion approach, the profile can progressively optimised by bracketing the ideal solution, and fabrication tolerance considerations can be incorporated into the design.

Fig.5 shows the Stokes parameters for each of the two guided modes of an asymmetric RIE-lag structure in the same GaAs/AlGaAs wafer structure at a wavelength of 1.064 $\mu$m examined previously. It is sufficient for a modal 3 dB splitter to incorporate a single slot; here we use dimensions of 0.10 $\mu$m wide and 0.27 $\mu$m deep taken from the RIE-lag calibration used in Ref. [2]. The averaged modal Stokes vectors bisect the angle between the axes in the $S_1$-$S_3$ plane: $\overline{\mathbf{S}}$ =(0.7294,0.6780,0) and (-0.7353,-0.6722,0) with effective indices $n_{\mathrm{eff}}$ =3.3356 and 3.3328 respectively, giving a half-beat length of 192.5 $\mu$m. These averaged modal Stokes vectors are reasonably close to the desired solution and further optimisation is possible with some fine-tuning of the rib dimensions.

The reproducability of the slot etch can be improved by incorporating an etch-stop layer instead of relying on a calibration of the RIE-lag effect, particularly where there is a doped upper cladding to provide a *p-i-n* structure for integration with lasers, amplifiers or modulators. Fig.6 shows the Stokes parameters for each of the two guided modes of an asymmetric RIE-lag structure in an idealised approximation to a commercial (IQE) aluminium quaternary 1.55 $\mu$m *p-i-n* laser wafer incorporating an etch stop layer [16]. The deep-etched rib width is 1.50 $\mu$m with 0.22 $\mu$m wide slot centred 0.39 $\mu$m from the edge of the rib. The averaged modal Stokes vectors bisect the angle between the axes in the $S_1$-$S_3$ plane as required: $\overline{\mathbf{S}}$ =(0.7025,0.7071,0) and (-0.6986,-0.7098,0) with effective indices $n_{\mathrm{eff}}$ =3.1503 and 3.1472 respectively, giving a half-beat length of 254.1 $\mu$m.

### 3.3. Differential Phase Shifter

In order to provide a variable polarisation transformation it is necessary to control the relative phase retardation between the two modes. As the beating between the modes transcribes an

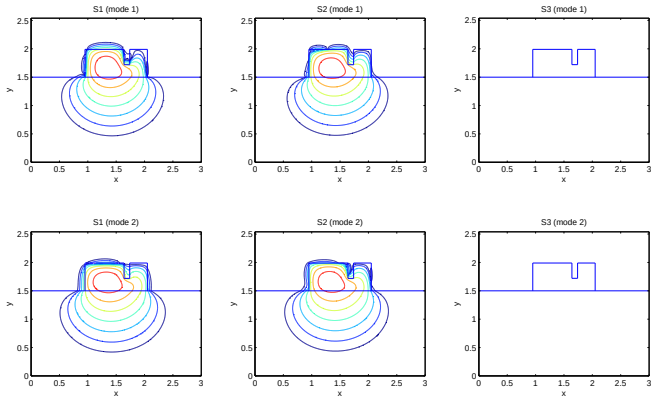


Fig. 5. The modulus of the Stokes parameters for the two guided modes at a wavelength of $\lambda$ =1.064 $\mu$m calculated using a full-vectorial modesolver. The 1.1 $\mu$m wide rib is composed of 0.49 $\mu$m thick GaAs on a $Al_{0.27}Ga_{0.73}As$ lower cladding with 0.10 $\mu$m wide slot centered 0.36 $\mu$m from the rib edge etched to a depth of 0.27 $\mu$m.

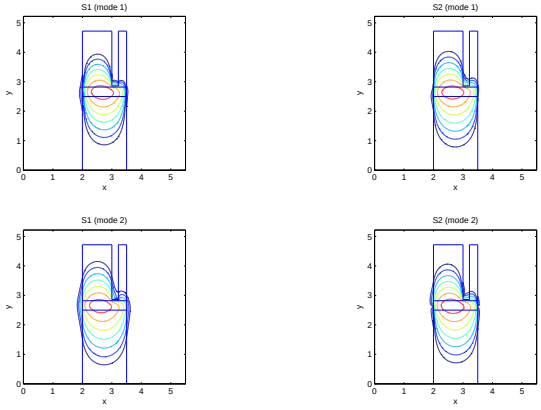


Fig. 6. The modulus of the Stokes parameters for the two guided modes at a wavelength of $\lambda$ =1.55 $\mu$m calculated using a full-vectorial modesolver. The structure is an idealised form of a commercial aluminium quaternary wafer with a 1.5 $\mu$m wide rib and a 0.22 $\mu$m wide slot centered 0.39 $\mu$m from the rib edge.

orbit around the modal axis, the differential phase shift determines the end point of this stage of evolution. Therefore the locus of output polarisation states from a differential phase shifter on the Poincaré sphere is a circular orbit, or part thereof. The simplest methods are based on a regular waveguide section which supports “TE-” and “TM-” polarised modes. In terms of evolution of the Poincaré sphere, such a differential phase retardation is represented by a specified rotation around the $S_1$ axis.

Most semiconductor waveguide modulation techniques give rise to anisotropic refractive index modulation. For example, a (multiple) quantum well structure will have the heavy-hole absorption feature in its spectrum for the TE-polarisation only, and therefore refractive index changes in the transparency region below the bandgap absorption edge will typically have a larger effect on TE-polarised modes in comparison to TM-polarised modes. Therefore a differential phase shift is normal for heterostructures employing the quantum-confined Stark effect [17], current injection of carriers, or even with a thermally-induced bandgap shift.

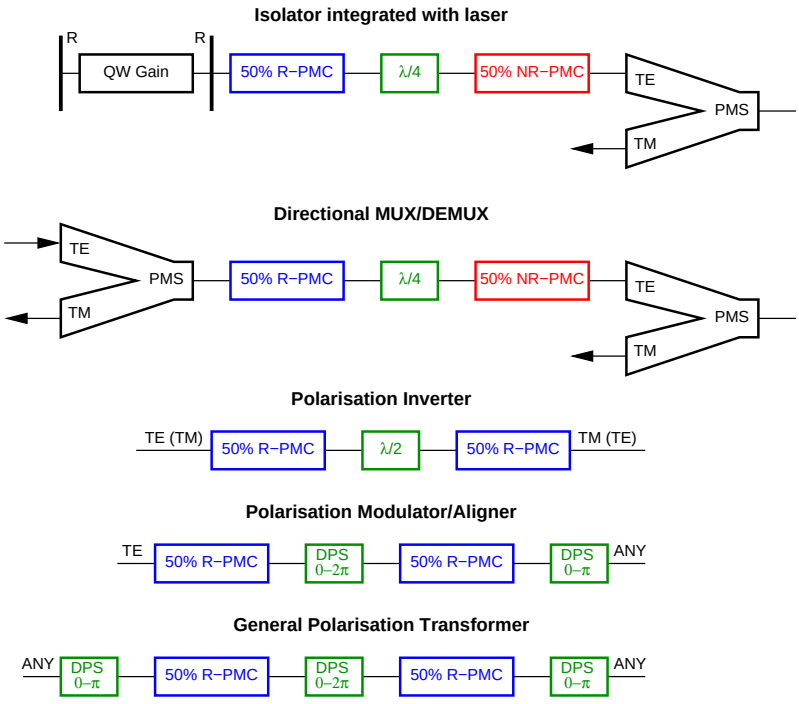


Fig. 7. Building blocks for integrated waveguide devices. Quasi-phase-matched nonreciprocal polarisation mode converter sections are shown in red, universal 3 dB reciprocal polarisation mode converter sections are shown in blue, and fixed or variable differential phase retarders are shown in green. Any additional polarisation discrimination is shown with schematic polarisation mode splitters (PMS) or a quantum well laser as examples.

In bulk cubic semiconductors the electro-optic (Pockels) effect can be used for high-speed modulation. The only non-zero electro-optic coefficient is $r_{41}$ (and equivalent) which means that for a voltage applied normal to the wafer surface, the phase-shift will be applied to TE-polarised modes only. Even when the material and the refractive index modification appear to be completely isotropic, the breaking of the symmetry by imposing a waveguide structure can result in a differential phase shift anyway. For example, consider the rib waveguide in Fig.2. The mode solver is repeated but with the room temperature bulk GaAs and AlGaAs refractive indices replaced with appropriate values for a temperature of 125°C. The modes now have effective indices $n_{\text{eff}}$ =3.3995 and 3.3913 respectively, giving a half-beat length of 65.10 $\mu$m. The mode profiles have been slightly modified so that the overlaps with low index cladding change. The reduction in the half-beat-length from 68.29 $\mu$m to 65.10 $\mu$m is indicative of a differential phase shift. It can be concluded that this is sufficient to provide a $\pi$ relative phase shift with a 100°C temperature rise in a waveguide length of 1.39 mm. Similar isotropic refractive index modulations can be achieved with the Franz-Keldysh effect (electric field) or bandfilling (carrier injection) [18].

## 4. Waveguide Device Integration

The mode-beating waveguide elements described previously, along with a polarisation mode splitter [19], [20] (equivalent of a polarising beam splitter) can be combined in a number of ways to provide functional polarisation devices as shown in Fig.7.

### *4.1. Optical Isolator*

The integrated optical isolator device contains a reciprocal and a non-reciprocal polarisation mode converter [5]. A quarter waveplate element is required between them to provide the required

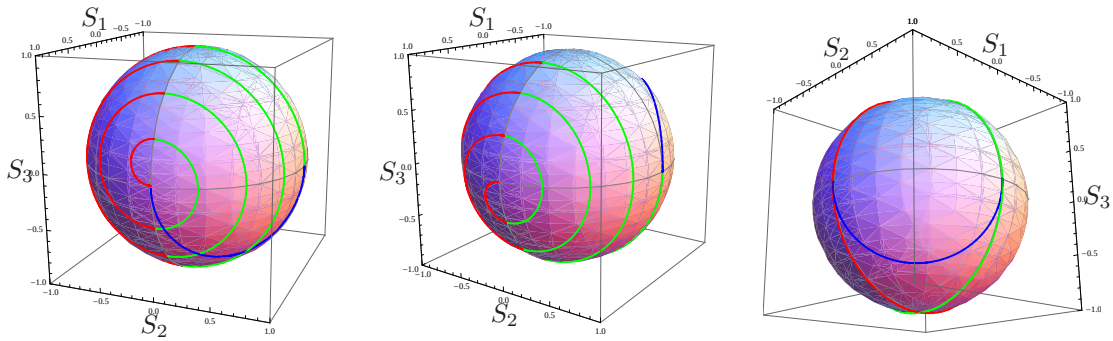


Fig. 8. Polarisation state evolution shown as trajectories from a launched TE-polarised mode on the modified Poincaré sphere (see text) for forward (left) and backward (centre) propagating light in the integrated optical isolator, and for the Polarisation Modulator device (right).

phase shift to convert linear to circular polarisation. The polarisation state evolution can be shown schematically as a trajectory on the Poincaré sphere as shown in Fig.8. In the forward propagation direction the initial TE-polarised guided wave $\overline{\mathbf{S}}$ =(1,0,0) undergoes (1) 3 dB reciprocal polarisation mode conversion (blue), (2) a quarter-wave phase retardation (green), and (3) a sequence of quasi-phase-matched half-beat lengths of magneto-optic (red) and half-wave phase retarders (green) to provide a TE-polarised output.

In the reverse direction note that the directions of the magnetic field and the asymmetry of the R-PMC are inverted with respect to the propagation direction so that the relevant modal axis are flipped: $(\Delta k_{\mathrm{brf}}, 0, \Delta k_{\mathrm{MO}}) \rightarrow (\Delta k_{\mathrm{brf}}, 0, -\Delta k_{\mathrm{MO}})$, and $(1/\sqrt{2}, 1/\sqrt{2}, 0) \rightarrow (1/\sqrt{2}, -1/\sqrt{2}, 0)$. An initial TE-polarised guided wave undergoes (1) a sequence of quasi-phase-matched half-beat lengths of magneto-optic (red) and half-wave phase retarders (green), (2) a quarter-wave phase retardation (green), and (3) 3 dB reciprocal polarisation mode conversion (blue) to provide a TM-polarised output $\overline{\mathbf{S}}$ =(-1,0,0).

This combined nonreciprocal polarisation mode conversion will provide optical isolator functionality with the incorporation of polarisation (TE/TM) discrimination at the input and output ports. This could be accomplished with polarisation mode splitters (which, more generally, provides a directional multiplexer/demultiplexer as shown in Fig.7) or anisotropic absorbers. If the output is into a polarisation preserving optical circuit, then there may not be a need for an output polarisation discriminator. If the optical input is from an integrated quantum well laser, then the TE-polarised output and the lack of heavy-hole features in the TM-polarisation spectrum may automatically provide the necessary polarisation selectivity (as shown in Fig.7).

### *4.2. Polarisation Modulator/Aligner*

A common method for obtaining optical amplitude modulation, particularly in integrated optics, is the Mach-Zehnder interferometer in which the light is split between two arms with a variable relative phase shift and recombined. Instead of using physically separate arms, the same principle can be applied where the two polarisation modes of a waveguide are used for the two distict optical paths. That is the amplitude in each mode of a waveguide can be modulated with a 3 dB reciprocal polarisation mode converter, a differential phase shifter and a second 3 dB reciprocal polarisation mode converter.

The polarisation state evolution for such a modulator with a TE-polarised guided-wave input is shown in Fig.8 (right). The first R-PMC rotates the polarisation state a half-turn around the $(1/\sqrt{2}, 1/\sqrt{2}, 0)$ axis from TE-polarised to 45° linearly polarised (blue). The differential phase shifter element then translates the polarisation state to a point on the locus of the $S_1$ =0 circle (green). The second R-PMC rotates the polarisation state a subsequent half-turn around the $(1/\sqrt{2}, 1/\sqrt{2}, 0)$ axis translating the locus of the polarisation state to the $S_2$ =0 circle (red). This range of polarisation states has a modulus ranging from 0 to 1 for the TE- and TM-polarised

components achieving amplitude modulation with a polarisation discrimination element. Reference [20] includes a schematic of such a polarisation-based amplitude waveguide modulator where the R-PMCs correspond to quarter-beat-length of 100% converters and the differential phase shift is provided by Pockel's electro-optic effect. A similar approach has also been described for a polarisation controller with cascaded elements consisting of orientated, spliced birefringent optical fibre sections and thermo-optic modulation [21].

The principal advantage of an amplitude guided-wave modulator based on polarisation manipulation over the standard Mach-Zehnder modulator is the single contiguous waveguide uses less real estate on the chip. It is therefore particularly suited to dense optoelectronic integration formats, such as in device arrays.

Returning to the polarisation state evolution in Fig.8 (right), with the Differential Phase Shifter element providing a phase difference in the range 0–$2\pi$ so that the locus of the potential polarisations is a complete circle, a second subsequent differential phase shifter element providing a phase difference in the range 0–$\pi$ would allow any point on the Poincaré sphere to be accessed. The schematic for such a polarisation modulator is shown in Fig.7. As this is a reciprocal device it can also be inverted to allow any inputed coherent polarisation state to be aligned to the TE-polarised mode (or alternatively the TM-polarised mode). Such a device would prove extrememly useful in providing dynamic control in a non-polarisation preserving network of polarisation sensitive components (such as semiconductor optical amplifiers).

For the case of a general polarisation transformer providing a conversion from any given coherent polarisation state into any other given polarisation state, this could be achieved with a back-to-back integration of two such modulators providing polarisation state alignment and subsequent modulation. However, such a device has a number of redundant elements which can be removed, namely two consecutive 3 dB reciprocal polarisation mode converter elements, and with their removal two consecutive differential phase shifter elements can be combined. The resulting minimum requirement for an any- to any-polarisation transformer consists of two 3 dB reciprocal polarisation mode converter elements and three differential phase shifter elements, as shown in Fig.7.

## 5. Conclusions

In this paper a number of III-V semiconductor based waveguide elements have been studied which can be combined to realise a range of polarisation functional devices. We have discussed, in particular, two classes of polarisation functional integrated waveguide devices, namely optical isolators (and related nonreciprocal devices), and polarisation modulators (and related reciprocal devices). All of the individual waveguide sections discussed here use the principal of mode-beating between the two fundamental polarisation modes of the waveguide. The difference between the types of section is the means by which a particular set of modes are obtained. The devices discussed here are generally formed as a single contiguous waveguide, although some nonreciprocal applications may additionally require a polarisation mode splitter. Therefore the devices discussed here are particularly suited to implementations where the tranverse chip real-estate is a constraint, such as in device arrays.

Both classes of devices require a reciprocal polarisation mode converter element(s) and we have identified that the requirements can be met with a universal 3 dB converter consisting of a half-beat-length (half-wave-plate equivalent) that provides 50% TE- to TM-polarisation (and TM- to TE-polarisation) conversion. Such a converter can be physically realised and we consider two single-trench asymmetric rib waveguide examples: 1064 nm application using RIE-lag and 1550 nm application using an etch-stop layer. The alternative 100% conversion solution that is discussed more prevalently in the current literature can only be approached asymptotically.

The nonreciprocal mode conversion discussed here is based on Faraday rotation in a garnet upper cladding. The form birefingence in a waveguide format prevents the required mode conversion from being achieved in a single step, but a quasi-phase-matched approach can be employed

with successive half-beat-lengths of magneto-optic and non-magneto-optic waveguide sections.

The waveguide analysis presented here is based on a full-vectorial finite-difference modesolver [4]. We observe that with typical III-V waveguide profiles of the scale of the vacuum wavelength on a semiconductor substrate, that the polarisation state has a only relatively small variation across the mode profile. Therefore it suffices to condense the polarisation state to an averaged Stokes vector. The validity of the approximation can be tested by the proximity of the modulus of the averaged Stokes vector to unity. We surmise that the validity of this approximation may be compromised for some nanophotonic wire (highly confined) structures. The use of an averaged Stokes vector allows some plane-wave constructs to be employed. We have used the Poincaré sphere to illustrate the polarisation state evolution in the integrated waveguide device designs.

## Acknowledgements

The authors acknowledge useful discussions with Dr. Marc Sorel.

## References

[1] A. Yariv, “Coupled-mode theory for guided-wave optics,” *IEEE J. Quantum Electron.*, vol. 9, pp. 919–933, 1973.
[2] B. M. Holmes and D. C. Hutchings, “Realisation of novel low-loss monolithically integrated waveguide mode converters,” *Photonics Tech. Lett.*, vol. 18, pp. 43–45, 2006.
[3] J. J. Bregenzer, S. McMaster, M. Sorel, B. M. Holmes, and D. C. Hutchings, “Compact polarization mode converter monolithically integrated within a semiconductor laser,” *J. of Lightwave Tech.*, vol. 27, pp. 2732–2736, 2009.
[4] A. B. Fallahkhair, K. S. Li, and T. E. Murphy, “Vector finite difference modesolver for anisotropic dielectric waveguides,” *J. Lightwave Technol.*, vol. 26, pp. 1423–1431, 2008.
[5] D. C. Hutchings, “Prospects for the implementation of magneto-optic elements in optoelectronic integrated circuits: a personal perspective (invited),” *J. Phys. D*, vol. 36, pp. 2222–2229, 2003.
[6] H. Yokoi, T. Mizumoto, and H. Iwasaki, “Nonreciprocal TE-TM mode converter with semiconductor guiding layer,” *Electronics Letters*, vol. 38, pp. 1670–1672, 2002.
[7] J. A. Armstrong, N. Bloembergen, J. Ducuing, and P. S. Pershan, “Interactions between light waves in a nonlinear dielectric,” *Phys. Rev.*, vol. 127, pp. 1918–1939, 1962.
[8] P. K. Tien, R. J. Martin, R. Wolfe, R. C. L. Craw, and S. L. Blank, “Switching and modulation of light in magneto-optic waveguides of garnet films,” *Appl. Phys. Lett.*, vol. 21, pp. 394–396, 1972.
[9] R. Wolfe, J. Hegarty, J. J. F. Dillon, L. C. Luther, G. K. Celler, and L. E. Trimble, “Magneto-optic waveguide isolators based on laser annealed (Bi, Ga) YIG films,” *IEEE Trans. Magn.*, vol. 21, pp. 1647–1650, 1985.
[10] B. M. Holmes and D. C. Hutchings, “Demonstration of quasi-phase-matched non-reciprocal polarisation rotation in III-V semiconductor waveguides incorporating magneto-optic upper claddings,” *Appl. Phys. Lett.*, vol. 88, p. 061116, 2006.
[11] V. P. Tzolov and M. Fontaine, “A passive polarization converter free of longitudinally-periodic structure,” *Optics Commun.*, vol. 127, pp. 7–13, 1996.
[12] J. Z. Huang, R. Scarrmozzino, G. Nagy, M. J. Steel, and R. M. Osgood, Jr., “Realization of a compact and single-mode optical passive polarization converter,” *IEEE Photon. Tech. Lett.*, vol. 12, pp. 317–319, 2000.
[13] L. M. Augustin, J. J. G. M. van der Tol, E. J. Geluk, and M. K. Smit, “Short polarization converter optimized for active-passive integration in InGaAsP-InP,” *IEEE Photon. Technol. Lett.*, vol. 19, pp. 1673–1675, 2007.
[14] E. D. Finlayson, J. M. Heaton, B. M. A. Rahman, and S. S. A. Obayya, “Polarization conversion in passive deep-etched GaAs/AlGaAs waveguides,” *J. Lightwave Technol.*, vol. 24, pp. 1425–1432, 2006.
[15] S.-H. Kim, R. Takei, Y. Shoji, and T. Mizumoto, “Single-trench waveguide TE-TM mode converter,” *Optics Express*, vol. 17, pp. 11 267–11 273, 2009.
[16] M. J. Strain, P. M. Stolarz, and M. Sorel, “Passively mode-locked lasers with integrated chirped bragg grating reflectors,” *IEEE J. Quantum Electron.*, vol. 47, pp. 492–499, 2011.
[17] D. A. B. Miller, D. S. Chemla, T. C. Damen, A. C. Gossard, W. Wiegmann, T. H. Wood, and C. A. Burrus, “Band-edge electroabsorption in quantum well structures: The quantum-confined stark effect,” *Phys. Rev. Lett.*, vol. 53, pp. 2173–2176, 1984.
[18] D. C. Hutchings, M. Sheik-Bahae, D. J. Hagan, and E. W. Van Stryland, “Kramers-Krönig relations in nonlinear optics,” *Opt. and Quant. Electr.*, vol. 24, pp. 1–30, 1992.
[19] L. M. Augustin, J. J. G. M. van der Tol, R. Hanfoug, W. J. M. de Laat, M. J. E. van de Moosdijk, P. W. L. van Dijk, Y.-S. Oei, and M. K. Smit, “A single etch-step fabrication-tolerant polarization splitter,” *J. Lightwave Technol.*, vol. 25, pp. 740–746, 2007.
[20] J. J. G. M. van der Tol, L. M. Augustin, A. A. M. Kok, U. Khalique, and M. K. Smit, “Use of polarization in InP-based integrated optics,” in *Conference on Lasers and Electro-Optics, San Jose, CA*. The Optical Society of America, 2008, p. CThM3.
[21] E. R. Lyons and H. P. Lee, “An electrically tunable all-fiber polarization controller based on deposited thin-film microheaters,” *IEEE Photon. Tech. Lett.*, vol. 14, pp. 1318–1320, 2002.